ELSEVIER

Journal of Marine Systems 30 (2001) 207–220

JOURNAL OF MARINE SYSTEMS

www.elsevier.com/locate/jmarsys

Small-scale temporal variations in biogeochemical features in the Strait of Gibraltar, Mediterranean side—the role of NACW and the interface oscillation

Fernando Gómez, Gabriel Gorsky [a], Laurent Striby [b], Juan M. Vargas [c], Nicolas Gonzalez [d], Marc Picheral [a], Jesus García-Lafuente [c], Manuel Varela [d], Madeleine Goutx [b,*]

[a] *Laboratoire d'Océanographie de Villefranche / mer, BP 28, 06234 Villefranche-sur-Mer, France*
[b] *Laboratoire de Microbiologie Marine, CNRS–INSU, UMR 6117, Université de la Méditerranée, Centre d'Océanologie de Marseille, Campus de Luminy, Case 907, 13288 Marseille Cedex 9, France*
[c] *Departamento de Física Aplicada II, Universidad de Málaga, 28071 Málaga, Spain*
[d] *Instituto Español de Oceanografía, Muelle de Animas s / n, 15001 A Coruña, Spain*

Received 4 January 2001; accepted 29 June 2001

Abstract

On the Mediterranean side of the Strait of Gibraltar, the distribution of physical, chemical and biological variables (temperature, salinity, nutrients, chlorophyll *a*, lipids, particles size and plankton abundance) was examined. Sampling was carried out between the surface and 150 m at a fixed station over a 24-h time series. The patterns observed were related to the overlaying of different processes. The Atlantic–Mediterranean interface acts as a strong pycnocline and its vertical oscillation accounts for the gross distribution of nutrients, particles, and living biomass. Injection of North Atlantic Central Water (NACW) into the upper layer occurs at the sill each semidiurnal tidal cycle (every 12 h). As a consequence, in the upper Atlantic layer the NACW was observed every 12 h in the trough of the interface oscillation, whereas Surface Atlantic Water (SAW) dominated in the crest at the fixed station. The initially nutrient-rich NACW was associated with eutrophic signatures such as high chlorophyll, large cells and low turbidity; The nutrient depleted SAW was associated with oligotrophic signatures such as low chlorophyll, small cells and high turbidity. The distribution of lipid biotracers at the depth of the chlorophyll maxima (10–40 m) depicted a similar trend with abundant chloroplast lipids and a low lipolysis index in NACW-enriched waters, and a high lipolysis index and abundant zooplankton tracers in SAW especially at night. During the eastward advection of Atlantic water, the nutrient content of NACW is likely to be assimilated by phytoplankton. A scenario is proposed for explaining changes in phytoplankton maxima composition during the time series observations, taking into account the timing of the NACW injection at the sill, the diurnal cycle and zooplankton grazing. Although more studies over a longer temporal scale are necessary to validate this scenario, our observations show the scale of daily variations in the physical/biological coupling in the Strait and the implications for nutrient and matter exchanges between the Atlantic and Mediterranean.

Keywords: Chlorophyll; Phytoplankton; Particles; Nutrients; Lipids; North Atlantic Central Water; Strait of Gibraltar

* Corresponding author. Tel.: +33-4-9182-9062; fax: +33-4-9182-9051.
E-mail addresses: fernando.gomez@fitoplancton.com (F. Gómez), goutx@com.univ-mrs.fr (M. Goutx).

0924-7963/01/$ - see front matter
PII: S0924-7963(01)00059-8

1. Introduction

The Strait of Gibraltar connects the Mediterranean Sea with the Atlantic Ocean. The exchange between the two basins is attributable to two opposite currents with a high-density contrast, modulated by tidal and subinertial variations (Candela et al. 1989; Bryden et al., 1994). Tidal ranges in the Gulf of Cádiz exceed 2 m, while in the Mediterranean Sea the range is less than 1 m. As a consequence, a drastic transition in the tides occurs within the Strait (García Lafuente et al., 1990; Candela et al., 1990). In the case of most tidal cycles, internal waves are generated by the interaction of the tidal flow with the prominent bottom features, particularly the Camarinal sill. The study of thermal microstructures has shown the high frequency of variability in the physical phenomena (e.g., Frassetto, 1960; Ziegenbein, 1970; Boyce, 1975; Lacombe and Richez, 1982).

Due to the considerable vertical exchange between the fresher inflowing Atlantic Waters (AW) and the saltier Mediterranean Outflowing Water (MOW), the region at the interface, between the two opposite currents, has been defined as a third layer with distinct properties (Bray et al., 1995). However, from the point of view of water exchange, the interface is the surface of null along-strait velocity. Therefore, it is possible to define the interface as a surface of a given salinity, whose mean depth coincides with that of the zero velocity (Bryden et al., 1994; García Lafuente et al., 2000).

The observed temperature and salinity distributions within the Strait can be attributed to the mixture of three principal types of water. On the Atlantic side of the Strait, Surface Atlantic Water (SAW) is warm and fresh and, as a result of atmospheric warming, forms a sharp seasonal thermocline (5 °C/100 m) above the colder and fresher North Atlantic Central Water (NACW). Below the Atlantic layer the cold, saline MOW is observed (Gascard and Richez, 1985; Ochoa and Bray, 1991). The properties of the water masses change along the Strait as a result of mixing, entraining and vertical advection (Bray et al., 1995). As the upper layer flows eastward, the mixing in the lower region erodes progressively at the NACW signature and the influence of SAW increases towards the top of the interface layer. The injection of NACW into the upper Atlantic layer of the Strait is highly influenced by tides and the amplitude of the internal waves (Gascard and Richez, 1985).

Although studies on the variability of physical phenomena have been frequent, the study of the biological features associated with them are less numerous. A few biological data are available from the Ictio. Alborán–Cádiz annual surveys (1993–1997) (Prieto et al., 1999; Rubín et al., 1999). On the Atlantic side, SAW forms an upper layer of low nutrient concentration, whereas the deeper NACW yields relatively high nutrient concentrations. Previously, Minas et al. (1991) reported the role of the entraining of NACW nutrients into the upper eastern Atlantic layer, as a factor introducing biological enrichment into the Strait and the Western Alboran Sea. Recently, within the context of the EC MAST3-CT96-0060 CANIGO (Canary Islands Açores Gibraltar Observations) project, new cruises in the area have been performed, including joint studies on biological, chemical and physical variables. These results show that the specific hydrodynamics of the Strait (especially the position of the interface) has a clear influence on biological variables. Phytoplankton biomass shows a tendency to increase towards the north eastern side of the Strait. This increase is directly related to the proximity of the interface average depth to the surface (Gómez et al., 2000a).

In this present study, we examined the short-term variability of chemical, biochemical and biological variables such as nutrients, lipids, chlorophyll *a*, plankton biomass and marine snow, over 24-h sampling on the Mediterranean side of the Strait of Gibraltar. This data set allows us to propose a conceptual scenario explaining the effects of the interface vertical oscillations on the injection and mixing of NACW in the inflowing Atlantic water, and ultimately on the periodicity of the distribution of biogeochemical variables.

2. Materials and methods

A 24-h survey was performed aboard R/V "Thalassa" (IFREMER-IEO, France–Spain) on September 8, 1997 (2 days before crescent moon). The sampled station was located at the eastern entrance of the Strait (36°02′N, 5°18′W; water depth was

about 800 m; Fig. 1). A CTD–rosette system equipped with 20-l Niskin bottles was used to collect water samples every 4 h (Table 1). Following this sampling, one or two casts were taken using the Underwater Video Profiler (Gorsky et al., 2000). This multisensor array includes a CTD probe, fluorometer, a nephelometer for turbidity measurements in a formazide turbidity unit (FTU) and a video system to estimate the abundance and size of particles > 500 μm.

The composition of the 0- to 400-m water column in the three water bodies (SAW, NACW and MOW) was estimated according to the method of Bray et al. (1995). Using the CTD–rosette data, we have calculated the depth-averaged values for temperature and salinity between 0 and 400 m at each casts. The composition of triangle apex points was (22.6 °C, 36.4) for SAW, (13.6 °C, 35.8) for NACW and (13.5 °C, 38.4) for MOW. The triangle formed by the three points enclosed all the measured *T*–*S* points during the sampling period at the fixed station.

Nitrate, phosphate and silicate were collected in 5-ml samples (unpreserved and stored at −20 °C) and analysed using a Technicon AA-II analyser following the method described by Grasshoff et al. (1983). For total chlorophyll and fractionated chlorophyll *a* analyses, suspended particles and particles larger than 20 μm were concentrated on GF/F filters by filtering 500 ml seawater samples and using particles retained when passing 2500 ml seawater through 20-μm filters, respectively. Filters were homogenized in a 90% acetone solution and kept overnight at 4 °C for pigment extraction. Fluorescence of the acetone extracts was measured using a Turner Designs-10 fluorimeter. Phaeopigments were estimated as the difference in fluorescence between acidified and non-acidified extracts (UNESCO, 1994). Lipids were extracted by concentrating suspended particles from 2 l seawater on GF/F filters according to the method of Bligh and Dyer (1959). The lipid extract was separated into the different class of compounds and analysed on an

Table 1
Date, time and tide (from Anuario de Mareas, 1997) during bottle sampling casts. All times were referred to the high water at Tarifa

Cast	Hour (GMT)	H/Tide
1	03:30	HW − 2
2	07:30	HW + 2
3	11:10	HW − 5
4	15:30	HW − 2
5	19:00	HW + 1.5
6	00:00	HW − 5

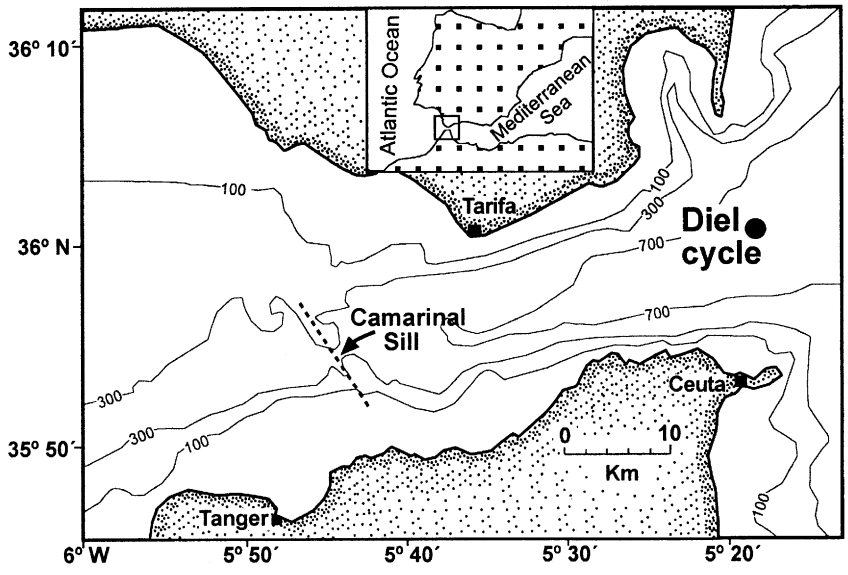

Fig. 1. Map of the Strait of Gibraltar and position of the diel cycle station sampled on September 8, 1997.

Iatroscan MK-IV apparatus following the protocol proposed by Gérin and Goutx (1994), modified by Striby et al. (1999). For microplankton analysis, 2 l of water was filtered through a 5-μm mesh collector and the retained material was washed out carefully with filtered seawater and then preserved with Lugol's solution. Subsamples (10–50 ml) were settled in Utermöhl chambers and counted using an inverted microscope. Simultaneously to the counting process, microplankton biomass expressed as biovolume was calculated by approximation to regular figures (ellipsoid, cylinder, hemisphere) using a VIDS V (Analytical Measuring Systems) semiautomatic image analysis system. Copepod abundance (including nauplii and juvenile stages) was estimated following the examination of the whole Utermöhl chamber, which uses 1–1.5 l of seawater. Although the counting error is $> 50\%$ according to the statistical considerations proposed by Lund et al. (1958), the pattern of abundance and distribution observed suffered no ambiguity and therefore has been reported. Due to shipboard constraint, only nutrients, pigments and biomass were collected from the first cast (03:30 GMT).

The Underwater Video Profiler (UVP) was used for the quantitative study of particles recording all objects illuminated in a 1.3-l volume. The lowering speed was 1 m s^{-1} and the analysed images did not overlap. The profiles obtained were digitized using a Matrox Magic digitizer (Matrox Electronic Systems) and analysed by the dedicated software (Gorsky et al., 2000; Stemmann et al., 2000). The tidal status during sampling was obtained from Anuario de Mareas (1997). All sampling times were taken according to High Water (HW hereafter) at Tarifa. The depth of the interface was considered as the isohaline of 37.8. This salinity was proposed by García Lafuente et al. (2000) based on their results of current meter mooring lines located at the eastern side of the Strait during the CANIGO period. The temporal evolution of different variables represented in the section plots was produced by interpolation between casts using the kriging as the gridding method in the Surfer software (Golden Software).

3. Results

3.1. Physical features

Fig. 2 shows that the composition of the water column changed during the 24-h cycle. Table 2 gives the percentage of the different water masses observed in the upper 400 m following the technique employed. The lowest salinity values were observed at 03:30 GMT at 45 m and were associated with the presence of relatively pure NACW. Later on, at 15:30 GMT, a new salinity minimum appeared. In both cases, the temperature was between 16 and 17 °C. At 07:30 and 19:00 h, respectively, the NACW

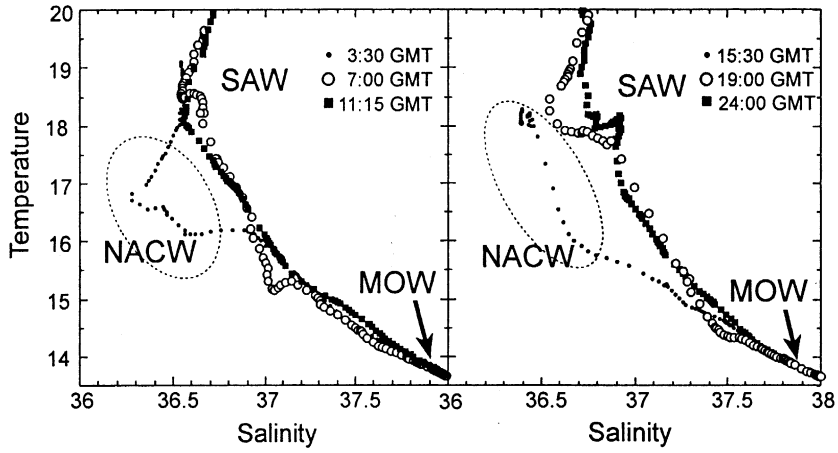

Fig. 2. Temperature (°C) and salinity diagrams from the CTD–rosette sampler system. The results showed lower salinity levels (NACW) approximately every 12 h. NACW, North Atlantic Central Water; SAW, Surface Atlantic Water; MOW, Mediterranean Outflowing Water.

Table 2
Percentage of SAW (Surface Atlantic Water), NACW (North Atlantic Central Water) and MOW (Mediterranean Outflowing Water) between 10-and 400-m depth calculated according to Bray et al. (1995). The percentages of Surface Atlantic Water and Mediterranean Outflowing Water do not present tidal modulations as clear as the percentage of North Atlantic Central Water

GMT hour	%SAW	%NACW	%MOW
03:30	17	6	77
07:30	15	4	82
09:30	15	1	84
11:10	15	1	85
12:30	21	2	77
15:30	17	6	77
19:00	16	1	83
00:00	22	1	77

signatures in the upper layer were still detected as a slight salinity minima (temperature about 18.5 °C) (Fig. 3B). The vertical oscillation of the interface and the presence of NACW in the upper layer were clearly related to the semidiurnal tidal cycle whereas the percentage of SAW and MOW water masses are not dependant on tidal modulations (Table 2). Evolution of the 14 °C isotherm was correlated to the oscillations at the interface, whereas oscillations of the near surface isotherms show the opposite pattern. Thus, the 20 °C isotherm was deeper when the interface was shallower. This feature can be associated to the NACW signatures.

The range of oscillations at the interface depth were around 30 and 40 m and reached a minimum depth (shallowest interface depth) about 2 h after High Water at Tarifa (HW + 2). These results agree with those of García Lafuente et al. (2000) who provide harmonic constants for the isohaline vertical oscillations as a function of salinity. Between 50 and 75 m, the vertical separation of the different isohalines was observed which was lowest at the time of the maximum height (wave crest) than at the minimum (wave trough). This behaviour is related to the vertical shear of velocities. When the shear is higher, the interfacial layer (defined as the separation between two given isohalines) is thicker. Since tidal

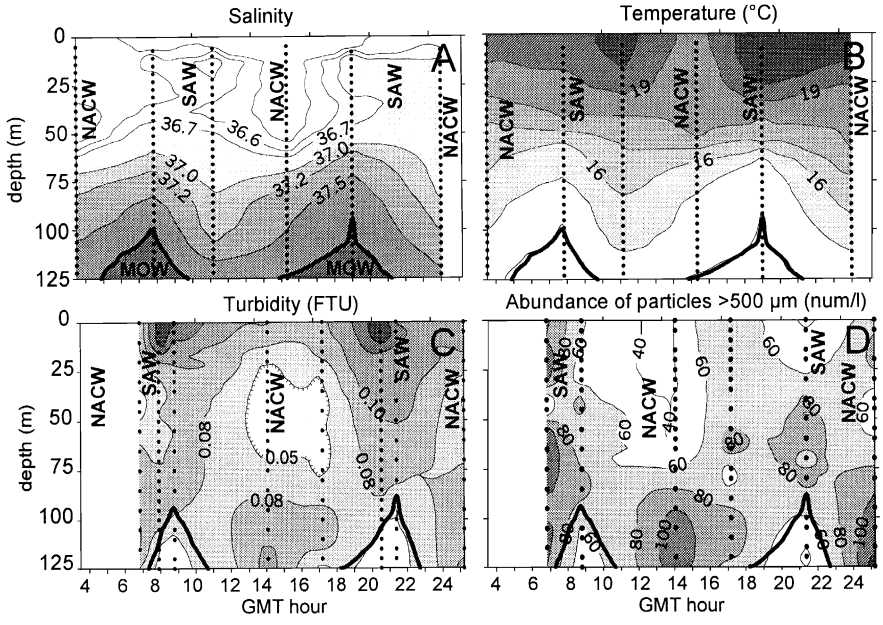

Fig. 3. Section plots of the upper 125 m at the diel cycle station. (A) Salinity, (B) temperature (°C), (C) turbidity (FTU) and (D) abundance of particles greater than 500 μm (number l^{-1}). Note that the shape of the interface in panel (A) and panels (C)–(D) are different. Salinity and temperature are taken from the CTD bottle and turbidity and particles from the Underwater Video Profiler using different casts. The identified water masses are noted on the diagram: NACW, North Atlantic Central Water; SAW, Surface Atlantic Water; MOW, Mediterranean Outflowing Water. The gross line represents the interface considered as the isohaline of 37.8.

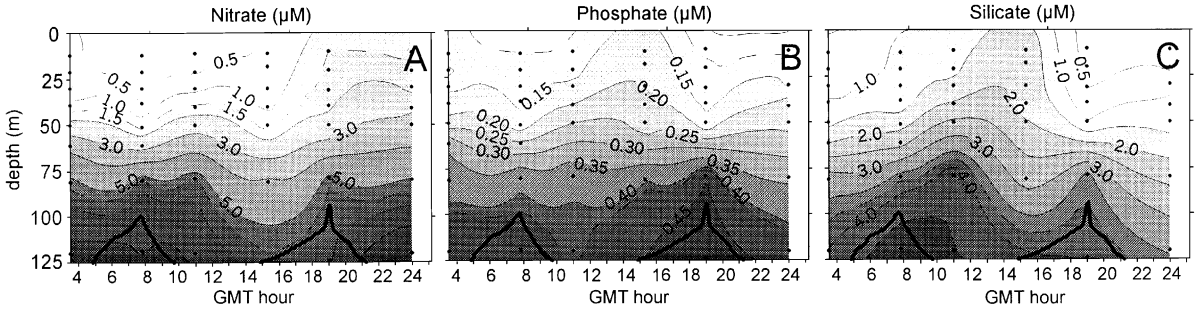

Fig. 4. Section plots of (A) nitrate (μM), (B) phosphate (μM) and (C) silicate (μM) distributions during the diel cycle. The gross line represents the interface as the isohaline of 37.8.

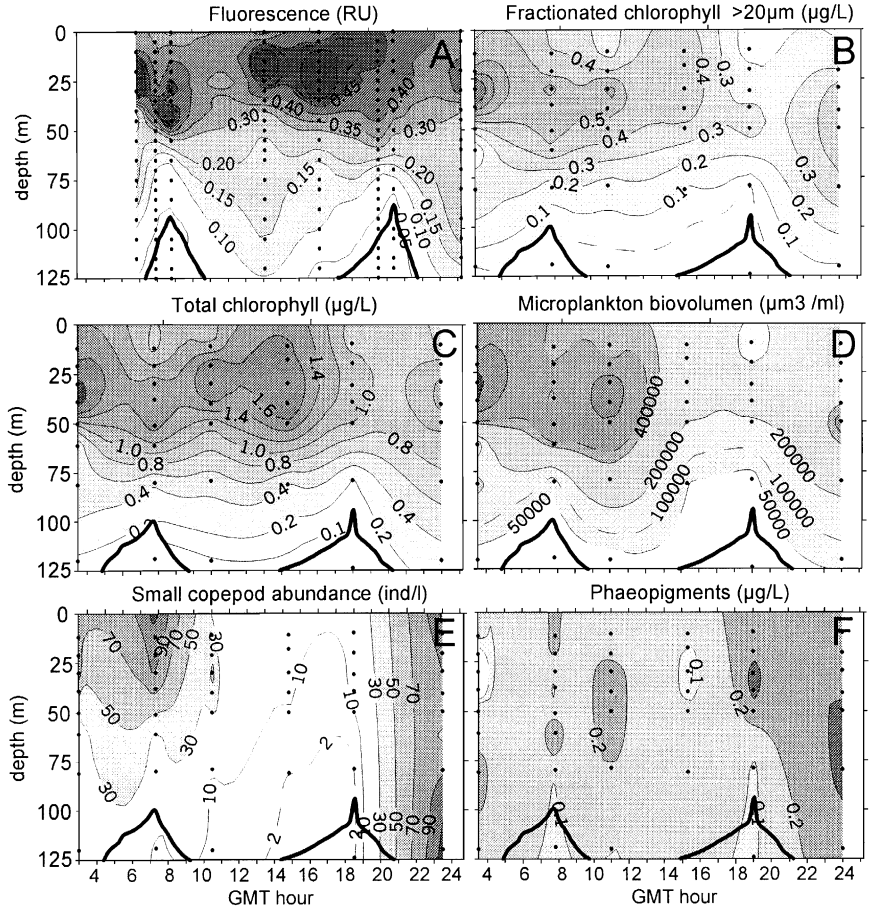

Fig. 5. Section plots of fluorescence (relative units, RU) from the (A) UVP fluorometer, (B) fractionated chlorophyll (from particles retained by a 20-μm pore size mesh, in $\mu g\ l^{-1}$), (C) total chlorophyll *a* ($\mu g\ l^{-1}$), (D) microplankton biovolume (> 500 μm^3, in $\mu m^3\ ml^{-1}$) from water samples, (E) abundance of copepods (individual l^{-1}) (mainly nauplii and juvenile stages), (F) Phaeopigments ($\mu g\ l^{-1}$). The gross line represents the interface as the isohaline of 37.8.

currents in the upper layer are small (García Lafuente et al., 2000), the shear is related to the inversion of the tidal currents in the lower layer, with a maximum current towards the Atlantic when the interface is at its lowest position. Therefore, the stratification is higher when the interface is shallower and the mixing is enhanced when it is deeper.

3.2. Particle distribution

The surface water turbidity (particles < 50 μm, units expressed as FTU) was high compared to the underlying water turbidity. Maximal values (0.18) were observed in waters associated with SAW signatures and exhibited the same pattern as the 20 °C isotherm, which depicted the crest of the interface oscillation. Turbidity values were lower in NACW. The abundance of large particles (> 500 μm) ranged between 10 and 120 particles l^{-1}. It was neither related to the chlorophyll biomass nor to nephelometry. Large particles (80–90 aggregates l^{-1}) accumulated above the interface in the 37.1–37.8 salinity gradient. Accumulation near the surface was noticeable in samples taken at night. Below the interface, in MOW, both variables presented low values (data not shown).

3.3. Nutrients

At the interface region (80–120 m), the distribution of nutrient concentration (Fig. 4), silicate in particular (Fig. 4C), was controlled by the interface oscillations, i.e. the shallower the interface depth, the shallower the nutrient maxima. On the contrary, the pattern observed for nutrient distribution near the surface was related to the presence of NACW signatures. The first salinity minimum (03:30 GMT) did not show any increase in nutrient concentration (Fig. 4) whereas the second salinity minimum (15:30 GMT) exhibited enhanced concentrations of phosphate and silicate. Nitrate concentrations showed the lowest values in the upper layer in the first hours of the diel cycle (Fig. 4A).

3.4. Phyto- and zooplankton biomass

At the interface region, in situ fluorescence (isoline 0.1) oscillated like the interface (Fig. 5A). The vertical distribution of both total and fractionated (> 20 μm) chlorophyll *a* were better related to fluorescence than to the interface oscillations. This might be due to the fact that Chl *a* data was obtained using discrete sampling (with only 1–2 samples in the interface region), whereas the spatial resolution of the fluorescence measurements was significantly higher. In the upper layer, fluorescence and total chlorophyll exhibited maxima in the 25- to 35-m layer associated with the NACW signature. High fluorescence and total chlorophyll *a* were also noticeable at 11:30. Total and fractionated chlorophyll *a* showed the highest value in the first maximum in the less saline water (at 03:30 GMT) and a second

Table 3
Lipid content and lipid class composition of suspended particles along depth (m) profiles. Total lipids (TL, μg/l), chloroplast lipids (Chlip, %), wax and sterol esters (WSE, %) and index of lipolysis (LI)

Time	Depth	TL	Chlip	WSE	LI
07:30	12	19.6	19.5	11.4	0.8
	21	5.5	13.3	6.5	2.2
	30	22.2	25.2	5.7	1.2
	38	19.2	17.3	43.1	0.5
	51	6.7	16.8	9.0	1.0
	80	4.7	16.7	14.9	0.2
	119	3.5	21.8	19.5	0.6
11:10	11	39.6	20.2	3.8	2.2
	30	22.8	24.5	4.2	1.4
	40	20.7	34.9	3.5	1.1
	80	29.2	30.0	10.3	1.2
	120	18.6	27.0	13.5	0.9
15:30	14	40.9	24.4	4.0	0.7
	31	22.0	43.4	7.5	0.4
	40	6.2	22.2	4.1	1.4
	81	21.7	29.6	4.6	1.8
	125	11.9	29.2	9.5	0.8
19:00	11	41.6	18.8	6.6	1.2
	31	16.5	19.9	7.3	1.2
	40	29.5	25.7	14.4	1.5
	80	18.3	29.1	12.4	1.4
	124	12.3	22.6	18.1	0.7
24:00	11	16.0	11.3	13.4	0.9
	29	20.1	11.0	7.4	3.0
	41	36.9	16.0	12.0	1.5
	79	13.3	14.5	9.5	1.1
	122	15.6	15.6	13.5	1.0

maximum at midday (15:30 GMT) (Fig. 5B–C). In the first maximum fractionated chlorophyll *a* (> 20 μm) represented about 40% of total Chl *a*, whereas in the second one the fractionated chlorophyll *a* represented 25–30% of the total Chl *a*. In the last sampling cast (24:00 GMT for bottle samples and 1:00 for UVP), an increase of fluorescence and chlorophyll suggested a third maximum.

The biovolume of larger phytoplankton (> 500 μm^3) ranged between 0.3 and 0.8 $mm^3\ l^{-1}$ (with maximum values corresponding to the first chlorophyll *a* maximum) and showed a slight oscillation with the interface (Fig. 5D). Microphytoplankton were mainly composed of colonial diatoms (> 80%), dinoflagellates and silicoflagellates. The first and third maxima were characterized by both small and large phytoplankton, whereas the second one in the middle of the day included smaller phytoplankton. These results are in good agreement with the distribution of fractionated chlorophyll (Fig. 5B–C).

The distribution of zooplankton (mainly small copepods) was neither directly related to the phytoplankton biomass maxima nor to the NACW lenses. Copepods showed the highest abundance during the night (Fig. 5E), being present in the upper layer at the end of the first night and in the whole water column at beginning of the second night of investigation. Abundant phaeopigments (Fig. 5F) were also observed during the second night of sampling.

3.5. Lipid signatures

Lipid classes can be used as tracers of organisms or of the biological activity associated with them. Total lipids (the sum of the different lipid classes in suspended particles) (3.5–41.5 μg l^{-1}) were accumulated in the surface layer in relation to the presence of planktonic biomasses and exhibited a minima at the level of the interface (Table 3 and Fig. 6A). A periodicity characterized the distribution of the individual components of the lipid pool. In surface waters, chloroplast lipids (Chlip), a tracer of phytoplankton cells (Parrish, 1988; Cailliau et al., 1999; Goutx et al., 2000), exhibited increasing contribution (Table 3) to total lipids from the beginning of the day through to midday (25.2% at 07:30, 34.9% at 11:10, 43.4% at 15:30). The Chlip maximum was associated with the 15:30 NACW lense above the trough of the interface oscillation (Fig. 6B). It then decreased to a minimum at night (24:00

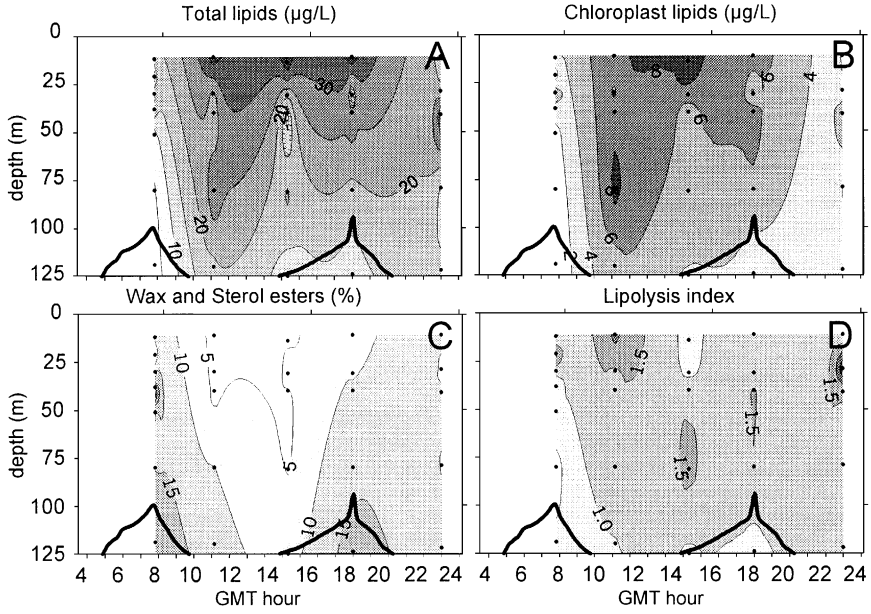

Fig. 6. Lipid biotracer distribution in suspended particles during the diel cycle. (A) Total lipids (μg l^{-1}), (B) the chloroplast lipids (μg l^{-1}), (C) the wax and sterol esters (%), (D) the lipolysis index. The gross line represents the interface as the isohaline of 37.8.

GMT). Wax esters and sterol esters (WE/SE), reserve products in zooplankton, are usually dominated by wax esters in marine samples (Parrish, 1988) and are found in zooplankton pellets, detritus and carcasses in marine suspended matter. At the surface, these zooplankton tracers exhibited a trend similar to that of small copepod abundance with higher contributions at night, in the 07:30 GMT (43%), 19:00 (14%) and 24:00 (13%) profiles, than during the day (11:10 and 15:30 profiles). Maxima were also observed at depth, in relation to the crest of the interface oscillation (Fig. 6C). The lipolysis index (LI) is the ratio of the lipid degradation metabolites to the entire acyl lipids such as wax esters and chloroplast lipids. It is an indicator of the early stage of organic matter degradation by heterotrophic hydrolytic activity. Weeks et al. (1993) found a relationship between LI and mesozooplankton grazing, whereas our experiments showed an increase of LI with increasing bacterial enzyme activity (Van Wambeke et al., 2001). The highest LI estimated in the surface layer during the time series were being observed at night (2.2 and 3.0 at 07:30 and 24:00, respectively) whereas the lowest value was associated with the NACW signature (0.4 at 15:30 GMT).

4. Discussion

Recent investigations have improved our knowledge of the water exchanges at Gibraltar, namely the effect of topographic constraints on the dynamics of the flow, the temporal variations of the exchanges and the effect of tides (Bryden et al., 1994; Send et al., 1999; García Lafuente et al., 2000; Tsimplis, 2000). By contrast, few studies have addressed the functioning of ecosystems in the Strait. One reason for this must be the difficulty in carrying out suitable sampling strategies for estimating biological processes when considering the spatial and temporal scales characteristic of this highly dynamic area. A preliminary step towards a comprehensive sampling program for biological studies in the Strait was performed in the framework of the CANIGO European program. Observations emphasized the heterogeneity of chemical and biological standing stocks in the area. However, quite permanent features in the distribution of biomass in summer (late June and early September) were related to the combined effect of the interface depth and the availability of light and nutrients on phytoplankton. Despite a certain variability in phytoplankton composition, a clear southwest/northeast gradient in autotrophic biomass, attributable to microphytoplankton, was observed (Gómez et al., 2000a) whereas the picoplankton contribution to the autotrophic biomass increased from Northeast to Southwest.

This work constitutes another approach to the spatio-temporal heterogeneity of the ecosystem components in the Strait. The time series observations lasted only 24 h due to inherent factors making sampling difficult in an area characterized by strong surface currents and winds (up to 25 m s^{-1} for the Levante), fishing activity and heavy ship traffic. However, for the first time, standing stocks of chemical, biochemical, and biological parameters were recorded at a fixed station in the Strait, simultaneously with the continual recording of the physical properties of the water masses.

4.1. Interface oscillations

Results show the relevant role of the interface oscillations, induced by the internal tide, by the distribution of chemical and biological variables. As already observed, the interface is the transition region between the nutrient-rich MOW and the relatively impoverished AW. In this region, the phytoplankton is produced and accumulates because of water stratification. The vertical displacement of the interface determines the position of the phytoplankton assemblages as well as the irradiance level required for primary production. Previous investigations performed at a northern station (Gómez et al., 2000a) in the Strait revealed a shallow interface which probably oscillated in the euphotic layer during the whole tidal cycle. As a consequence, the phytoplankton received a continuous supply of nutrients from MOW and enough irradiance for photosynthetic production, generating a large abundance of biomass. At the site investigated during our 24-h survey, the interface oscillated between 100 and 140 m so the irradiance level was only sufficient to support a low phytoplankton biomass.

The role of the interface as a density gradient is also relevant for the vertical distribution of both small and large particles. Small particles appeared to

be mainly produced in the productive surface waters and remained concentrated herein, whereas, large particles (> 500 μm) accumulated at the deeper salinity gradients above the interface (Fig. 3). Large particles are formed through the aggregation of small particles (phytoplankton and/or detritus) into faecal pellets and mucous (Alldredge and Silver, 1988). Aggregation might also occur through coagulation by physical processes (Fowler and Knauer, 1986; Alldredge and Gotschalk, 1989). Both processes are likely to occur in the Strait. In the surface layer at night, the lipid signatures of the zooplankton corresponded to large particle accumulation and certainly reflect the formation of aggregates through zooplankton feeding activity. In addition, the periodic variation of the shear stress of velocities during the tidal cycle (Bray et al., 1990), is likely to generate aggregation of particles produced in the water overlying the upper region of the interface. Finally, the surface of zero velocity also resides inside the region of the interface. Here, phytoplankton cells and detritus are not so rapidly advected as observed in the upper and lower layers, leading to an increased residence time of particulate organic matter of photosynthetic origin.

4.2. Tidal periodicity of NACW injection

Besides horizontal stratification, our results demonstrate that above the interface region, the distribution of biological variables is related to the presence and the proportion of NACW. Gascard and Richez (1985) reported that this occurs only during neap tides when a high proportion of NACW can enter the eastern entrance of the Strait; The mean amplitude of the internal waves is weaker and the interface is not reaching the bottom at the sill as it happens during a spring tide. Injection of NACW through the Strait can be followed during the ebb tide, and salinity levels lower than 36.0 can be detected at Low Water. During spring tides, the amplitude of the internal waves is greater than for neap tides, a strong mixing occurs at the location of NACW and this water mass is not observed in the *T–S* diagrams. During our survey, the quantity of NACW injected at the sill was clearly controlled by the semidiurnal tidal periodicity (Table 2). Recently Tsimplis and Bryden (2000) also reported the influence of the diurnal component on the intrusion of NACW. At the sill the NACW lenses appear around 130–140 m depth with higher signatures each two tidal cycles associated with the deeper interface values. Using chemical tracers, Elbaz-Poulichet et al. (2001) reported an average value of 3% for the NACW in the Atlantic inflow.

A clear turbidity minima corresponded to the NACW signatures (Fig. 3C). Jerlov (1953) also reported a minimum value for turbidity in the NACW layer in the Gulf of Cadiz when compared to the SAW. This low turbidity can be related to the position of NACW in the water column in the Gulf of Cadiz. Indeed, considering that the distribution of suspended matter strongly relates to the production of living matter and derived detritus, low particle content might be expected in NACW located in the aphotic zone in the Cadiz Gulf. By contrast, the SAW located in the euphotic zone presented high concentrations of small particles originating from biological activity. Although the concentration of particles in the NACW increased along the Strait, it did not reach the values observed in the biologically ageing SAW.

On the Atlantic side, NACW is relatively rich in nutrients in comparison with the impoverished SAW (Gómez et al., 2000b). Increased proportions of initially nutrient-rich NACW in surface waters obviously enhanced phytoplankton biomass. Signatures of a freshly upwelled system (low turbidity, large cells, chloroplast lipid maxima, minimum of lipid hydrolysis tracer, low phaeopigment levels) accompanied this feature. On the contrary, signatures of zooplankton biomass and hydrolysis activity predominated in SAW (Figs. 5E and 6D, Table 3) with maxima registered in the night samples. These signatures are certainly the result of the different heterotrophic status of the SAW and NACW, with the aged SAW having a more developed heterotrophy than the freshly upwelled NACW.

4.3. Diel pattern

In contrast to the trend above, NACW-enriched surface waters exhibited different nutrient concentrations and zooplankton distributions, not always fitting the tidal-related semi-diurnal periodicity. In the first hours of the cycle (03:30 GMT), the NACW

signature was nutrient depleted but included high phytoplankton biomass, leading to the conclusion that nutrients were depleted due to the biological uptake. By contrast, in the second signature (at 15:30), we observed a relatively large concentration of nutrients, in particular silicate and phosphate (Fig. 4) associated with a greater number of smaller cells. Generally, nitrate is consumed faster than silicate or phosphate during the development of a bloom (Kudo et al., 2000). Differences in light available to microalgae growing in NACW lenses, might explain the different nutrient contents. NACW lenses exposed to the light would favour intense photosynthetic activity. Lower nutrient uptake would occur in NACW lenses exposed to less illumination, so the development of a strong phytoplankton maximum could not be completed.

Zooplankton distribution seems related to the normal pattern of diel vertical migration (Lampert, 1989). The low number of copepods in NACW-enriched surface water during the day suggests that this population migrates to the aphotic zone during the day to avoid visual predators (Zaret and Suffern, 1976). By contrast at night, copepod activity at the surface was noticeable by the increase in marine snow accompanied by zooplankton lipid tracers of biomass (cf. Fig. 6C) and/or activity (cf. Fig. 6D and Table 3). Indeed, zooplankton activity can contribute to the formation of large particles via the production of rapidly sinking faecal material (Karl et al., 1988; Kiorboe, 1997). This was particularly true for the last maximum (24:00 GMT) which associated large copepod abundance to high phaeopigment levels from the surface down to the depth of the interface (Fig. 5F).

4.4. Conceptual scenario

The Strait presents an assemblage of inter-related physical phenomena which control biological processes. Isolating one of these physical phenomena is necessary to understand the observed periodicity of chemical and biological variables. In this study, we aimed to emphasize the role of the injection of nutrient-rich NACW into the upper inflowing Atlantic layer by mixing at the sill.

Previously, Gómez et al. (2000a) reported a recirculation scheme for diatoms at the Strait including (i) the development of important biomasses at the northeastern part of the Strait where the interface is shallower, (ii) sinking through the interface region, (iii) transport to the west in outflowing waters and (iv) subsequent injection in the upper Atlantic waters at the sill when outflowing waters meet high bottom features. Processes of advection and mixing are known to favour the growth of taxa such as diatoms, especially adapted to mixing events compared to other groups. It is likely that seeding cells show higher growth rates in the nutrient-enriched NACW than in the nutrient depleted SAW.

Based on this assumption, we propose a scenario of the history of each NACW signature along the Strait that could explain the observed distributions of chemical and biological parameters (Fig. 7). We estimate an average velocity in the upper layer (35–40 cm s^{-1}) from the ratio between the mean transport (0.7–0.8 Sverdrup (Sv)) (1 Sv = 10^6 m^3 s^{-1}) (Bryden et al., 1994; García Lafuente et al., 2000) and the mean cross-section (about 2 km^2). This estimation falls within the values reported by Send et al. (1999) for the eastern side of the Strait. Considering that the Camarinal sill is the place where the deep NACW can ascend and that its distance to the diel cycle station is about 40 Km, the time needed for the ascending water to reach the station is approximately 27–30 h.

The frequent high interface oscillations at the sill (Pettigrew and Needell, 1989; Wesson and Gregg, 1994; Bray et al., 1990, 1995) are controlling the proportion of NACW injected into the Atlantic inflowing waters. The tidal-related interface oscillation is based on the model proposed by Armi and Farmer (1988) and La Violette and Arnone (1988). For neap tides, authors have reported the maximum AW inflow at the sill just before Low Water and the minimum just before High Water. Considering that the injection of nutrient-rich NACW occurs with a frequency of 12 h, and that this water is advected towards the Mediterranean Sea in the euphotic zone, we can observe two phytoplankton maxima capable of nutrients uptake for growth each day.

Due to alternating day and night, one of these phytoplankton blooms receives a lower light irradiation than the other. As a consequence, on the Mediterranean side, one of these phytoplankton maxima has low nutrient and high phytoplankton biomass

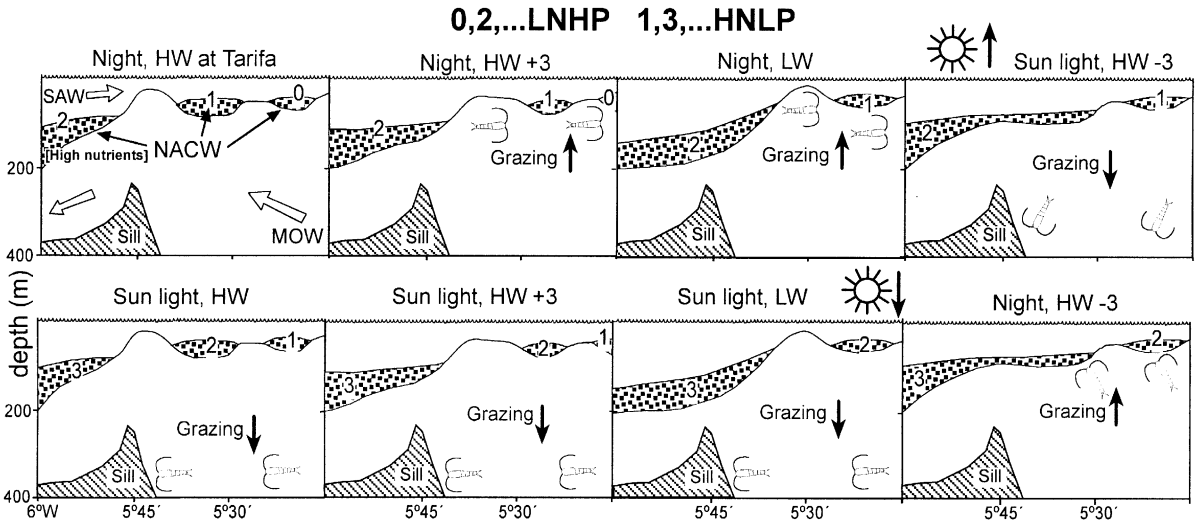

Fig. 7. Scheme proposed to explain the sequence of biological maxima and associated nutrient signatures in the Mediterranean side of the Strait of Gibraltar during a one day period. Nutrient-rich NACW is injected into the inflowing Atlantic Water at the Camarinal sill every semidiurnal tidal cycle around Low Water (LW). Sampling times are taken according to the High Water (HW) at Tarifa. The position of the diel cycle station is the right side of each panel. There are 40 km between the sill and the station. Typically, the scenario is as follows: NACW nutrient-enriched lense 1 upwelled for example at midday at the sill, earlier than the start of the scenario (on the left), is transported eastwards during the night and submitted to zooplankton grazing before reaching the fixed station in the middle of the following day (cf. 15:30 NACW lense). NACW-enriched lense 2 upwelled around midnight, supports phytoplankton growth mostly during the illuminated period and under low grazing pressure before reaching the fixed station in the middle of the following night (cf. 3:30 NACW lense). The periodicity of NACW injection coupled to the diel pattern of biological processes (phytoplankton growth versus zooplankton grazing) lead to different types of NACW-enriched lenses transported from the Atlantic to the Mediterranean. Lense 1 has high nutrient and low phytoplankton maxima (HNLP) (with relatively few microphytoplankton cells in it) and lense 2 has low nutrients and high microphytoplankton maxima (LNHP) when reaching the fixed station (36°02′N, 5°18′W).

(LNHP) whereas the next maximum has the opposite characteristics (HNLP). In this study, the NACW signature observed at the diel cycle station at 03:30 GMT (first salinity minimum) probably upwelled 27–30 h before this time and thus, had developed a phytoplankton maxima in an illuminated period during its eastward advection. Moreover, considering that the distribution of copepods in surface waters (cf. Fig. 5E) and associated tracers (Fig. 6C) showed higher values during the night, for each day, one of the maxima could be more affected by grazing than the other. Copepods would preferentially consume larger cells (microphytoplankton). Therefore, one day, a maxima can show less microphytoplankton (chlorophyll in particles > 20 μm) than the next. Such phenomenon would affect pico- and nanophytoplankton to a lesser extent.

According to the proposed scenario, the proportion of NACW in each tidal cycle, despite its low contribution to the AW (Table 2), appears as an important factor in determining the intensity of the chlorophyll maxima observed at the eastern side of the Gibraltar Strait. Phenomena such as the entraining of outflowing Mediterranean water or the passage of the internal bore were not considered, but certainly must be taken into account in the modulation of the biological consequences of the injection of NACW. Obviously other constituents of the tide, especially the fortnightly variations can alter the proposed scheme. Further studies in the area will be necessary to test this preliminary model and factors affecting its variability.

Acknowledgements

This work was supported by the Commission of the European Communities Marine Science

and Technology (MAST III) Program under contract MAST3-CT96-0060 (CANIGO project). All CANIGO partners involved in WP4.2 are gratefully acknowledged for their efficient and friendly contribution over the period of the program. We thank L. Prieto for her chlorophyll data, R. Carballo for her help in nutrient analysis and the crew of the R/V "Thalassa" for their assistance.

References

Alldredge, A.L., Gotschalk, C., 1989. Direct observations of the mass flocculation of diatom blooms: characteristics, settling velocities and formation of diatom aggregates. Deep-Sea Res. 36, 159–171.

Alldredge, A.L., Silver, M.W., 1988. Characteristics, dynamics and significance of marine snow. Prog. Oceanogr. 20, 41–82.

Anuario de Mareas, 1997. Instituto Hidrográfico de la Marina, Ministerio de Defensa, Cádiz, Spain.

Armi, L., Farmer, D.M., 1988. The flow of Mediterranean Water through the Strait of Gibraltar. (also entitled: Farmer, D.M. and Armi, L. The flow of Atlantic water through the Strait of Gibraltar) Prog. Oceanogr. 21, 1–105.

Bligh, E.G., Dyer, W.J., 1959. A rapid method of total lipid extraction and purification. Can. J. Biochem. Physiol. 37, 911–917.

Boyce, F.M., 1975. Internal waves in the Strait of Gibraltar. Deep-Sea Res. 22, 597–610.

Bray, N.A., Winant, C.D., Kinder, T.H., Candela, J., 1990. Generation and kinematics of the internal tide in the Strait of Gibraltar. In: Pratt, L.J. (Ed.), The Physical Oceanography of Sea Straits. Kluwer Academic Publishing, Norwell, MA, pp. 477–491.

Bray, N.A., Ochoa, J., Kinder, T.H., 1995. The role of the interface in exchange through the Strait of Gibraltar. J. Geophys. Res. 100, 10775–10776.

Bryden, H.L., Candela, J., Kinder, T.H., 1994. Exchange through the Strait of Gibraltar. Prog. Oceanogr. 33, 201–248.

Cailliau, C., Belviso, S., Goutx, M., Bedo, A., Park, Y., Charriaud, E., 1999. Sedimentation pathways in the Indian sector of the Southern Ocean during a production regime dominated by regeneration. Mar. Ecol. Prog. Ser. 19, 53–67.

Candela, J., Winant, C., Bryden, H.L., 1989. Meteorologically forced subinertial flows through the Strait of Gibraltar. J. Geophys. Res. 94, 12667–12674.

Candela, J., Winant, C., Ruiz, A., 1990. Tides in the Strait of Gibraltar. J. Geophys. Res. 95, 7313–7335.

Elbaz-Poulichet, F., Morley, N.H, Beckers, J.M., Nomerange, P., 2001. Metal fluxes through the Strait of Gibraltar: the influence of the Tinto and Odiel rivers SW Spain. Mar. Chem. 73, 193–213.

Fowler, S.W., Knauer, G.A., 1986. Role of large particles in the transport of elements and organic compounds through the oceanic water column. Prog. Oceanogr. 16, 141–156.

Frassetto, R.A., 1960. A preliminary survey of thermal microstructure in the Strait of Gibraltar. Deep-Sea Res. 7, 152–162.

García Lafuente, J.M., Almazán, J.L., Castillejo, F., Khribeche, A., Hakimi, A., 1990. Niveau de la Mer dans le détroit de Gibraltar: Marées. Rev. Hydrogr. Int. Monaco 67, 113–132.

García Lafuente, J., Vargas, J.M., Plaza, F., Sarhan, T., Candela, J., Bascheck, B., 2000. The tide at the eastern section of the Strait of Gibraltar. J. Geophys. Res. 105, 14197–14214.

Gascard, J.C., Richez, C., 1985. Water masses and circulation in the Western Alboran Sea and in the Strait of Gibraltar. Prog. Oceanogr. 15, 157–216.

Gérin, C., Goutx, M., 1994. Iatroscan-measured particulate and dissolved lipids in the Almeria–Oran frontal system. J. Mar. Syst. 5, 343–360.

Gómez, F., Echevarría, F., García, C.M., Prieto, L., Ruiz, J., Reul, A., Jiménez-Gómez, F., Varela, M., 2000a. Microplankton distribution in the Strait of Gibraltar: coupling between organisms and hydrodynamic structures. J. Plankton Res. 22, 603–617.

Gómez, F., González, N., Echevarría, F., García, C.M., 2000b. Distribution and fluxes of dissolved nutrients in the Strait of Gibraltar and its relationships to microphytoplankton biomass. Estuarine Coastal Shelf Sci. 51, 439–449.

Gorsky, G., Picheral, M., Stemmann, L., 2000. Use of the Underwater Video Profiler for the study of aggregate dynamics in the North Mediterranean. Estuarine Coastal Shelf Sci. 50, 121–128.

Goutx, M., Momzikoff, A., Striby, L., Andersen, V., Marty, J.C., Vescovali, I., 2000. High frequency fluxes of labile compounds in the central Ligurian Sea, northwestern Mediterranean. Deep-Sea Res. I 47, 535–558.

Grasshoff, K., Erhardt, M., Kremling, K., 1983. Methods of Seawater Analysis. 2nd edn. Verlag Chemie, Weinheim, 419 pp.

Jerlov, N.G., 1953. Particle distribution in the ocean. Rep. Swed. Deep-Sea Exped. 3, 73–97.

Karl, D.M., Knauer, G.A., Martin, J.H., 1988. Downward flux of particulate organic matter in the ocean: a particle decomposition paradox. Nature 332, 438–441.

Kiorboe, T., 1997. Small-scale turbulence, marine snow formation, and planktivorous feeding. Sci. Mar. 61, 141–158.

Kudo, I., Yoshimura, T., Yanada, M., Matsunaga, K., 2000. Exhaustion of nitrate terminates a phytoplankton bloom in Funka Bay, Japan: change in SiO_4: NO_3 consumption rate during the bloom. Mar. Ecol. Prog. Ser. 193, 45–51.

Lacombe, H., Richez, C., 1982. The regime of the Strait of Gibraltar. In: Nihoul, J.C.J. (Ed.), Hydrodynamics of Semi-enclosed Seas. Elsevier, Amsterdam, pp. 13–73.

Lampert, W., 1989. The adaptative significance of diel vertical migration of zooplankton. Funct. Ecol. 3, 21–27.

La Violette, P.E., Arnone, R.A., 1988. A tide-generated internal waveform in the western approaches to the Strait of Gibraltar. J. Geophys. Res. 93 (C12), 15653–15667.

Lund, J.W.G., Kipling, C., Le Cren, E.D., 1958. The inverted microscope method of estimating algal numbers, and the statistical basis of estimation by counting. Hydrobiologia 11, 143–170.

Minas, H.J., Coste, B., Le Corre, P., Minas, M., Raimbault, P., 1991. Biological and geochemical signatures associated with the water circulation through the Strait of Gibraltar and in the western Alboran Sea. J. Geophys. Res. 96, 8755–8771.

Ochoa, J., Bray, N.A., 1991. Water mass exchange in the Gulf of Cadiz. Deep-Sea Res. 38, S465–S503.

Parrish, C.C., 1988. Dissolved and particulate marine lipid classes: a review. Mar. Chem. 23, 17–40.

Pettigrew, N.R., Needell, G.L., 1989. Flow structure and variability in the Tarifa Narrows section of the Strait of Gibraltar. In: Almazán, J.L., Bryden, H., Kinder, T., Parrilla, G. (Eds.), Seminario Sobre la Oceanografía Física del Estrecho de Gibraltar. SECEG, Madrid, pp. 207–229.

Prieto, L., García, C.M., Corzo, A., Ruiz Segura, J., Echevarría, F., 1999. Phytoplankton, bacterioplankton and nitrate reductase activity distribution in relation to physical structure in the northern Alboran Sea and Gulf of Cádiz (southern Iberian Peninsula). Bol. Inst. Esp. Oceanogr. 15, 401–411.

Rubín, J.P., Cano, N., Prieto, L., García, C., Ruiz, J., Echevarría, F., Corzo, A., Gálvez, J.A., Lozano, F., Escánez, J., Vargas, M., Hernandez, F., 1999. The structure of the pelagic ecosystem related to oceanographic and topographic features in the Gulf of Cádiz, Strait of Gibraltar and Alboran Sea (NW sector) during July 1995. Inf. Téc. Inst. Esp. Oceanogr. 175, 1–73.

Send, U., Font, J., Krahmann, G., Millot, C., Rhein, M., Tintoré, J., 1999. Recent advances in observing the physical oceanography of the western Mediterranean Sea. Prog. Oceanogr. 44, 37–64.

Stemmann, L., Picheral, M., Gorsky, G., 2000. Diel changes in the vertical distribution of suspended particulate matter in the NW Mediterranean Sea investigated with the Underwater Video Profiler. Deep-Sea Res. I 47, 505–531.

Striby, L., Lafont, R., Goutx, M., 1999. Improvement in the Iatroscan thin-layer chromatography-flame ionisation detection analysis of marine lipids. Separation and quantitation of mono- and diacylglycerols in standards and natural samples. J. Chromatography A. 849, 371–380.

Tsimplis, M.N., 2000. The vertical structure of tidal currents at the Camarinal sill at the Strait of Gibraltar. J. Geophys. Res. 105, 19709–19732.

Tsimplis, M.N., Bryden, H.L., 2000. Estimation of the transports through the Strait of Gibraltar. Deep-Sea Res. I 47, 2219–2242.

UNESCO, 1994. Protocols for the Joint Global Ocean Flux Study (JGOFS) core measurements. Man. Guides 29, 1–170.

Van Wambeke, F., Goutx, M., Striby, L., Sempéré, R., Vidussi, F., 2001. Short-term variability of heterotrophic bacteria at a fixed station in the Ligurian Sea (Western Mediterranean): relationships with microbial food web structure, dissolved organic matter and non living particulate organic carbon. Mar. Ecol. Prog. Ser. 212, 89–105.

Weeks, A., Conte, M.H., Harris, R.P., Bedo, A., Bellan, I., Burkill, P.H., Edwards, E.S., Harbour, D.S., Kennedy, H., Llewellyn, C., Mantoura, R.F.C., Morales, C.E., Pomroy, A.J., Turley, C.M., 1993. The physical and chemical environment and changes in community structure associated with bloom evolution: the Joint Global Flux Study North Atlantic Bloom Experiment. Deep-Sea Res. 40, 347–368.

Wesson, J.C., Gregg, M.C., 1994. Mixing at Camarinal Sill in the Strait of Gibraltar. J. Geophys. Res. 99, 9847–9878.

Zaret, T.M., Suffern, J.S., 1976. Vertical migration in zooplankton as a predator avoidance mechanism. Limnol. Oceanogr. 21, 804–813.

Ziegenbein, J., 1970. Spatial observations of short internal waves in the Strait of Gibraltar. Deep-Sea Res. 17, 867–875.